

Ultrasound and Conventional Synthesis of CeO₂/ZnO Nanocomposites and Their Application in the Photocatalytic Degradation of Rhodamine B Dye

Nidhi Shah¹, Karan Bhangaonkar¹, Dipak V. Pinjari² and Shashank T. Mhaske^{1*}

¹ Department of Polymer and Surface Engineering, Institute of Chemical Technology, Matunga, Mumbai - 400 019, India

² Chemical Engineering Department, Institute of Chemical Technology, Matunga, Mumbai - 400 019, India
Email: stmhaske@gmail.com

Abstract. CeO₂/ZnO composite nanoparticles are synthesized by using in-situ precipitation method, without any stabilizers, via conventional i.e. non-ultrasound (NUS) and ultrasound-assisted processing technique (US). The structure, morphology, particle size and % weight loss of the synthesized nanoparticles were analyzed by using X-ray powder diffraction (XRD), Thermogravimetric Analysis (TGA), Scanning electron microscopy (SEM) and Transmission electron microscopy (TEM) to establish the formation of core shell type nanomaterials with an average particle size under 15 nm. The effectiveness of the synthesized core shell morphology of CeO₂/ZnO (catalyst) for the photocatalytic degradation of Rhodamine B (RhB) dye has also been investigated. It has been observed that the catalysts prepared by sonochemical method exhibit higher photocatalytic activity as compared to the catalysts prepared by the conventional method. It was also found that the ultrasound-assisted technique is an energy efficient method as it saves more than 80% of energy along with a substantial reduction in reaction time, as compared to conventional synthesis technique.

Keywords: Sonochemical method, CeO₂/ZnO composite nanoparticles, Particle size, Dye degradation

1 Introduction

Dyes and modified dyestuff chemicals are commonly found in large quantities in the effluents of textile, paper, leather, cosmetics industries. After processing these chemicals, the associated wastewater effluents mix with water bodies upon disposal causing environmental and health related hazards.[1] Certain dyes are potentially carcinogenic and toxic in nature and hence, researches have paid much attention into developing photocatalytic materials that efficiently degrade the dye.[2] Semiconductor mediated photocatalysis has emerged as an important destructive technology leading to the mineralization of most of the organic pollutants. Many reports have been made to study the photocatalytic activity of different semiconductors such as ZnO, ZrO₂, Fe₂O₃, CdS and SnO₂ [3]. The coating of inorganic nano-sized material with another inorganic material to form core-shell type nanostructures has become an important route for synthesis of composite materials. Photocatalytic activity of a core material can be increased by coating it with a more active shell material.

Ceria i.e. cerium dioxide (CeO₂) has received more attention in recent years due to many distinctive characteristics, such as unique ultraviolet radiation absorbing ability [4], high stability at higher temperature, high hardness index and its reactivity [5]. However, CeO₂ is generally not considered as a photoactive material [6]. Also, the poor thermal stability of pure CeO₂, has limited its application in oxygen storage. To overcome this problem, some strategies have been adopted like mixing with metal or metal oxide to increase the thermal stability. On the other hand ZnO based materials are used in many fields, because of the photocatalytic nature, low cost and environmental sustainability.[7] ZnO being an important semiconductor catalyst, it is used in many applications as photocatalyst[8-11].

Recently, researchers have paid much attention to CeO_2/ZnO composite for potential applications [12-17]. $\text{CeO}_2\text{-ZnO}$ composite nanofibers were fabricated via the electrospinning technique and then studied for its photocatalytic behaviour [12]. Well-dispersed $\text{CeO}_2\text{-ZnO}$ composite fabricated through a simple chemical reaction followed by annealing treatment exhibited enhanced activity for CO oxidation [13]. S. Prabhu synthesized $\text{CeO}_2\text{-ZnO-TiO}_2$ semiconductor composites by sol-gel method and photocatalytic activity of the synthesized composite for the degradation of Rhodamine B (RhB) under visible light irradiation was investigated [14]. Sensors based on cerium oxide-zinc oxide ($\text{CeO}_2\text{-ZnO}$) composites were fabricated by using thick-film screen printing of hydrothermally grown powders and they are used as sensor element for ethanol sensor related applications [15]. Wet-chemical precipitation route was used to prepare radical-shaped ZnO micro prisms and to deposit cerium oxide (CeO_2) on the surface of ZnO, to form CeO_2/ZnO microstructures and their photocatalytic activity was studied [16]. CeO_2/ZnO nanostructured microspheres with an average diameter of about 3.8 μm were synthesized by a solid-stabilized emulsion route. These are used as catalysts for the oxidative coupling of methane with carbon dioxide, the conversion of methane corresponded with that using the CeO_2/ZnO nanoparticles [17]. Different chemical methods are used for the synthesis of CeO_2/ZnO composites, such as atmospheric pressure metal-organic chemical vapour deposition (AP-MOCVD) [18], hydrothermal synthesis [19], soft solution chemical route [20], solid-stabilized emulsion route [21], sol-gel method [22] and precipitation technique [23]. Enomoto and co-workers have successfully coated magnetite nanoparticles with silica using the Sonochemical method. Also, Gedanken and co-workers have succeeded in depositing magnetite nanoparticles on silver surface using the sonochemical technique [24]. Enterzari and co-workers have recently reported the coating of cadmium sulfide with titanium dioxide by the sonochemical method [25].

Semiconductor mediated photocatalysis has been investigated extensively as a viable technique for the removal of organic and inorganic pollutants from aqueous streams. The technique has been proven effective for the oxidative destruction of recalcitrant organic compounds such as dyes [26]. Rhodamine B (RhB) is widely used as a colorant in textiles and food industry but it is harmful to the human beings and animals. Considering the hazardous nature and harmful effects of Rhodamine B efforts have been made to degrade RhB using composite nanoparticles [27].

In this work we are aiming to coat CeO_2 with ZnO by in-situ chemical reaction via both sonochemical (US) assisted and conventional (NUS) methods. Herein we aim to investigate the photocatalytic activity of the prepared composite nanoparticles for degradation of Rhodamine B dye. Also, we are further investigation the role of ultrasound on the reaction time and yields of the products when compared to the conventional method.

2 Paper Preparation

2.1 Materials

Zinc acetate dihydrate [$\text{Zn}(\text{CH}_3\text{COO})_2 \cdot 2\text{H}_2\text{O}$] and Cerium nitrate hexahydrate [$\text{Ce}(\text{NO}_3)_2 \cdot 6\text{H}_2\text{O}$] precursor were obtained from S. D. Fine Chemicals Ltd., Mumbai, India. Sodium hydroxide [NaOH] was obtained from Merck Ltd., Mumbai, India. Rhodamine B dye was procured from Shah Enterprises, India. Deionized water was used for all the dilution and sample preparation. All chemical reagents are analytical grade and directly used as purchased, without further purification.

Ultrasound setup:

For sonochemical synthesis technique, the ultrasound was generated with the help of a horn type ultrasonic instrument set up [34]. The schematic of the setup is given in Fig. 1. The specification and details of the setup, processing parameters used during the experiments are: Make: Ace, USA, operating frequency: 22 kHz, rated output power: 750 W, diameter of stainless steel tip of horn: 1.3×10^{-2} m, surface area of ultrasound irradiating face: 1.32×10^{-4} m², expected ultrasound intensity: 3.4×10^5 W/m².

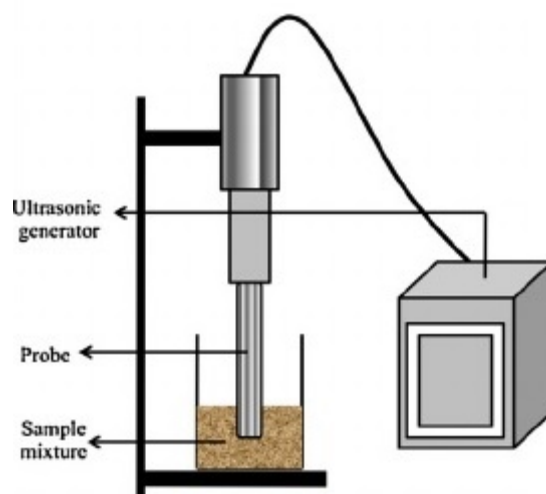


Figure 1. Ultrasound equipment set up.

2.2 Synthesis of CeO₂/ZnO Composite Nanoparticles via Conventional Method (NUS)

The synthesis of core-shell type CeO₂/ZnO nanoparticles was carried out via conventional precipitation method, followed by a typical procedure, 1.5 g (0.1 gmol) of Ce(NO₃)₂ · 6H₂O was dissolved in 50 ml of deionized water-ethanol matrix (equal volumes) and 0.6 g, (0.3 gmol) sodium hydroxide was also dissolved in 50 ml of deionized water-ethanol matrix. Both mixtures were mixed together using dropwise addition. The reaction was allowed to proceed for 4 hrs at 35 ± 2°C. To this solution, 2.2 g (0.2 mol) of Zn(CH₃COO)₂ · 2H₂O in 50 mL of deionized water-ethanol matrix (equal volumes) was added dropwise, stirring was continued for 10 more minutes. An equal molar amount of sodium hydroxide in another deionized water-ethanol matrix was prepared and added to the above colloidal solution drop by drop with continuous stirring at 80°C. The reaction was continued for 1 hr with the formation of ZnO shell by precipitation mechanism. We have repeated the reaction procedure and concluded that the reaction time to form shell is 1 hr. The solution was centrifuged at 10,000 rpm for 10 minutes to separate the product and the settled product was washed several times with deionized water and ethanol to remove the byproducts. After complete washing, the product was dried in a hot air oven at 120°C for 3 hrs.

2.3 Synthesis of CeO₂/ZnO Nanoparticles via Ultrasound Assisted Method (US)

The synthesis of core-shell type CeO₂/ZnO nanoparticles via ultrasound assisted precipitation method followed a typical procedure; 1.5 g (0.1 gmol) of Ce(NO₃)₂ · 6H₂O was dissolved in 50 ml of deionized water-ethanol matrix (equal volumes) and 0.6 g, (0.3 gmol) sodium hydroxide was also dissolved in 50 ml of deionized water-ethanol matrix (equal volumes) and kept ready. The sodium hydroxide solution was then added dropwise to the cerium nitrate hexahydrate solution under sonication using an Ultrasonic Horn (ACE 22 kHz) at 40% amplitude for 2 min with a 5 s pulse and 5 s relaxation cycle at time t = 0 h. Care was taken to see to it that the addition was done in conjunction with the sonic pulse afforded by the transducer (Horn). After addition of sodium hydroxide, it was again exposed to acoustic cavitation (by using ultrasonic horn) for further 18 min, by keeping all sonication parameters constant (same as that was used during mixing), to carry out the complete reaction of cerium nitrate hexahydrate with sodium hydroxide. The temperature of the reaction mixture was maintained at 35 ± 2 °C by circulating water in a jacketed reactor which was used for synthesis. To this solution, 2.2 g (0.2 mol) of Zn(CH₃COO)₂ · 2H₂O in 50 mL of deionized water-ethanol matrix (equal volumes) was added dropwise under sonication was continued for 2 more minutes. An equal molar amount of sodium hydroxide in another deionized water-ethanol matrix (equal volumes) solution was prepared and added

to the above colloidal solution and sonication drop by drop at room temperature. The sonication was continued for a total of 8 minutes with the formation of ZnO shell by precipitation mechanism. The solution was centrifuged at 10,000 rpm for 10 minutes to separate the product, and the settled product was washed several times with deionized water to remove the byproducts. After complete washing, the product was dried in a hot air oven at 120°C for 3 hrs.

2.4 Photocatalytic Activity Measurements

The photocatalytic activity of the CeO₂/ZnO composite particles synthesized by both US and NUS techniques was evaluated by the degradation of aqueous solutions of Rhodamine B (RhB) dye using a photoreactor. The photoreactor is a closed box with a UV lamp Spectroline XX-15 N which emits radiation at 365 nm with intensity of 2000 W/cm². The RhB dye solution with a concentration of 25 ppm was prepared for each experiment, in order to compare the activity of CeO₂/ZnO photocatalysts synthesized by US and NUS methods. The photocatalytic reaction was carried out at constant concentration of photocatalysts in each case. The experiments were performed with different amounts showed that the photocatalytic degradation ratios of Rhodamine B rapidly increased with the increase of nano-sized catalyst powder up to 0.05% and then the degradation of Rhodamine B reached a constant value for any additional amount of catalyst. A constant concentration of photocatalysts at 0.05% was hence maintained during the degradation experiment. Solutions with 50 mg of photocatalysts made via US and NUS techniques, suspended in 100 ml dye solution were prepared to make 0.05% aqueous solution respectively. The suspension was subjected to irradiation under UV-vis light for a span of 90 minutes. Prior to photoreaction, the suspension was magnetically stirred in dark condition for 30 min to establish absorption/desorption equilibrium condition. Also, during the photocatalytic reaction, the aqueous suspension was magnetically stirred. The solutions were exposed to ambient temperature of 35 °C and pH of 7 was maintained during the process. Aliquots of the mixture were taken out with using micropipette at periodic intervals during the irradiation. These samples were subjected to an ultracentrifuge in order to separate any suspended solids and then analysed in the double beam UV-vis spectrophotometer. The wavelength of maximum absorbance (λ_{max}) of dye was found to be 554 nm. Reproducibility of the obtained experimental data is important in investigating the effects of the operating parameters. In the current work, all the experiments were carried out three times to estimate the reproducibility of the obtained data. The graphs were plotted using mean values obtained from the data.

3 Characterizations

The phase structures of CeO₂/ZnO nanoparticles were studied on a Rigaku Mini-Flex X-Ray Diffractometer instrument using CuK α radiation source ($\lambda=0.154$ nm). XRD patterns were recorded at angles between 2° and 80°, with a scan rate of 2°/min. Particle sizes were determined using the Debye-Scherrer equation. The thermal behavior of the composite CeO₂/ZnO particles was investigated by using thermogravimetric analysis. The method used a Q50 TGA with standard furnace. The TGA investigation was carried out at a temperature ramp of 20°C/min, from ambient temperature (25 °C) till 1000°C. The morphology and diameter of individual nanoparticles were characterized by a JEOL, JSM-6380 LA 15kV scanning electron microscope. The morphology of core-shell CeO₂/ZnO nanoparticles and diameter of core and thickness of shell were characterized by Philips Model CM200 Transmission Electron Microscope having an operating voltage from 20kV to 200kV with the resolution of 2.4 Å⁰. The photocatalytic and sonocatalytic degradation of RhB dye, using the synthesized particles as catalyst, was investigated using a Perkin-Elmer UV-visible Spectrophotometer. Demineralized water was used as a blank reference.

4 Results and Discussions

4.1 Reaction Yield

The reaction time taken for conventional synthesis of CeO₂ core was 4 hrs and for coating it with ZnO shell to form CeO₂/ZnO core-shell composite nanostructures was 1 hr. Hence, the total time for conventional synthesis of the composite particles was 5 hrs (300 min). For ultrasound assisted synthesis of CeO₂ core, 20 min of sonication was required and a further sonication of 10 mins was required to coat it with the ZnO shell. Hence, a total time of 30 mins was required for the ultrasound assisted synthesis of CeO₂/ZnO core-shell composite nanostructures. It was found that these reaction times were optimum for the respective reaction and no further increase in % yield was observed on increasing the reaction time. The percentage yield of the reaction was estimated based on the initial weight of the raw materials taken and final weight of the product obtained after the complete drying (compared to the stoichiometrically expected quantity). Since, the composite particles were washed after synthesis with deionized water; the unreacted raw materials as well as any byproducts formed were separated and removed during this step. It was observed that yield of the reaction in the case of ultrasound-assisted technique (US) for synthesis of CeO₂/ZnO particles was $68.53 \pm 1\%$ and that in case of conventional synthesis technique (NUS) was $51.28 \pm 1.8\%$. The yield from ultrasound-assisted technique (US) is thus higher than conventionally (NUS) synthesized CeO₂/ZnO particles. The error (\pm variation) is less than 2% for conventionally (NUS) synthesis and 1% for ultrasound-assisted (US) synthesis technique.

Ultrasound can induce unique high energy chemistry through the process of acoustic cavitation: the formation, growth, and implosive collapse of bubbles in a liquid, which can create extreme conditions in localized, short lived hot spots. Bubble collapse in liquids results in an enormous concentration of energy from the conversion of the kinetic energy of liquid motion into heating of the contents of the bubble. The high local temperatures and pressures, combined with extraordinarily rapid cooling, provide a unique means for driving chemical reactions under extreme conditions. The possible reason behind the increase in the yield in less time is due to the formation of hotspots and rapid micro-mixing generated by acoustic cavitation. The yield is increased by 20% with a saving of 270 min reaction time. Sonication also causes a reduction in the average particle size of the composite material (Table 1). Fast kinetics of the US reaction do not provide enough time for particle nucleation and growth, which is the probable reason for a reduced average particle size.

The calculation in terms of total energy consumed by ultrasound and conventional method were done by several researchers. [28- 32] It has been reported that ultrasound method for synthesis of core shell nanoparticles is energy efficient, energy required to synthesize per unit weight of CeO₂/ZnO is 18 (kJ/gm) for US method and 140 (kJ/gm) for conventional method. Thus, US approach proved to be energy efficient as it has saved more than 80% of energy utilized by conventional method and also reduction in reaction time.

Table 1: Average crystal size and % crystallinity of US synthesized CeO₂, ZnO, CeO₂/ZnO and NUS synthesized CeO₂/ZnO composite

Sr No	Sample	Average crystal size d nm	Average % crystallinity
1	CeO ₂ US	55.09	13.69
2	ZnO US	43.63	26.18
3	CeO ₂ /ZnO US	21.18	19.6
4	CeO ₂ /ZnO NUS	26.41	24.25

4.2 X- Ray Diffraction (XRD)

The phase identification and structural changes were investigated with the help of X-Ray diffraction (XRD) technique. Figure 2 shows the typical XRD patterns recorded over 20°-80° for all the synthesized samples, which gives a good insight into the crystallinity of the products. It was observed that there are two sets of diffraction peaks for the CeO₂/ZnO sample, which indicated that the synthesized samples were composite materials. Figure 2 shows the XRD patterns for the CeO₂/ZnO nanoparticles

synthesized by both US and NUS techniques. The XRD peaks at 2θ 28.541°(111), 33.071°(200), 47.471°(220), 56.331°(311), 59.071°(222) and 69.401°(400) are attributable to CeO₂. The contribution of ZnO was attributed to the peaks with 2θ at 31.86° (100), 34.54° (002), 36.32° (101), 47.62° (102), 56.66° (110), 62.96° (103), 68.04° (112), and 69.18° (201). The diffraction peaks are consistent with (JCPDS Card No. 34-0394) for CeO₂ and (JCPDS Card No. 36-1451) for ZnO. Crystallite size and % crystallinity of the material can also be computed using the XRD patterns.

XRD patterns of synthesized CeO₂/ZnO composite nanostructures for both US and NUS process exactly match with one another. The crystallite size for US technique was 21.18 nm and that for NUS technique was relatively larger, at 26.41 nm. Table 1 summarizes the crystallite sizes and % crystallinity observed in the CeO₂/ZnO composite core-shell particles formed via US and NUS techniques.

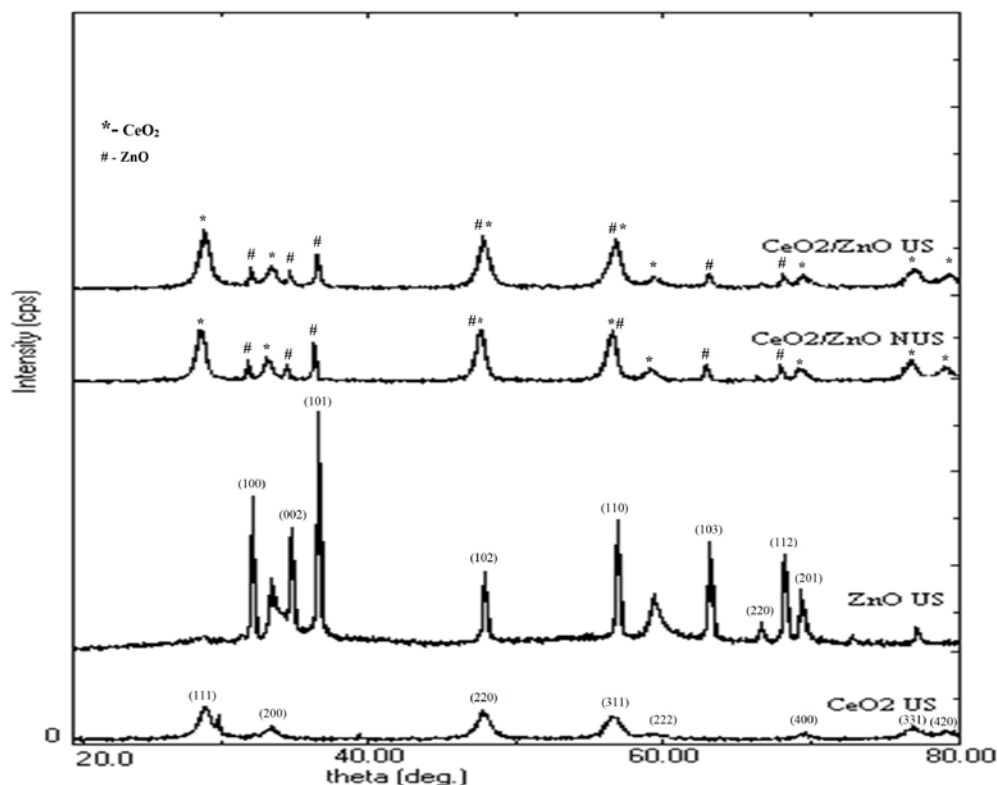


Figure 2. XRD plot of US synthesized CeO₂, ZnO, CeO₂/ZnO and NUS synthesized CeO₂/ZnO.

4.3 Thermogravimetric Analysis

The thermal behaviour of the composite CeO₂/ZnO particles synthesized by conventional as well as ultrasound-assisted techniques was investigated by using thermogravimetric analysis. Figure 3 shows the weight loss for US and NUS techniques. It was observed that continuous weight loss occurred for both samples. At 75°C, it was observed that the weight loss for CeO₂/ZnO composite particles synthesized by US technique and NUS technique were 1.15% and 0.05% respectively. As the samples were heated further, a notable weight loss was observed at 145 °C, which was 7.01% for US and 0.6% for NUS technique. This weight loss can be attributed to the dissociation of free and physically adsorbed water molecules on the nanoparticles. On heating the samples further, another notable weight loss was observed at 315°C, which was 17.03% for US and 4.58 % for NUS technique. The possible reason for this reduction in weight may be the loss of chemisorbed water molecules and loss of OH⁻ ions from the structure. At 595°C, the final weight loss of US and NUS synthesis techniques were observed to be 21.48% and 6.92%, respectively.

Use of ultrasound assisted technique causes a change in the crystallography of the nanoparticles. Formation of hotspots during acoustic cavitation and micro-mixing leads to an increase in the brownian motion of molecules. This does not allow the formation of a regular crystal structure during the core-shell particle synthesis, which leads to a reduced thermal stability of the particles synthesized using ultrasound assisted (US) technique, which is confirmed by a higher weight loss as compared to the NUS technique. Another reason for the higher weight losses exhibited by the particles synthesized using the US technique may be that sonication causes a reduction in the average particle size, which increases the efficiency of thermal conduction. Hence, at a lower temperature US particles will undergo thermal convective currents, which may cause a phase transformation, thus leading to the significant weight loss [33]. Further investigations may be carried out to conclude the aforementioned. Ultrasound enhanced high intensity collisions occurring between particles dispersed in the solution may lead to water condensation reaction as reported by Enomoto et al [34] and Frost et al [35]. The observation of higher weight loss in the case of US synthesized sample could be due to this phenomenon as well.

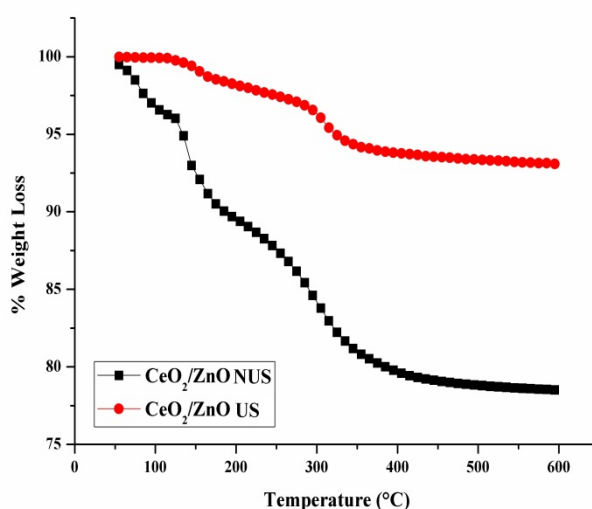


Figure 3. TGA curves of US and NUS synthesized CeO_2/ZnO nanoparticles

4.4 Scanning Electron Microscopy (SEM)

Scanning Electron Microscopy (SEM) was carried out to provide evidence to the morphology of the composite CeO_2/ZnO nanoparticles synthesized via US and NUS techniques. The morphology, size and structure of the particles have been investigated in detail using SEM. Figure 4 shows the SEM micrographs of CeO_2/ZnO nanoparticles synthesized using conventional and ultrasound-assisted techniques respectively. The micrographs of the synthesized particle support the observations from the XRD patterns. The US synthesized CeO_2/ZnO particles show a substantially smaller particle size. The US synthesized particles also show more dispersion and considerably lower agglomeration when compared to the NUS synthesized particles indicating sonication effect.

Use of ultrasound-assisted technique for synthesis of CeO_2/ZnO composite nanoparticles not only reduces the time required for the reaction but also influences in there action step by considerably reducing the particle size and increasing the packing of the particles as surface area is increased. This increases the surface area of particles synthesized via US technique, which effectively improves the materials properties. This very idea is used in our research to establish the superiority of ultrasound-assisted technique over conventional technique to synthesize core-shell particles for application as photocatalytic materials.

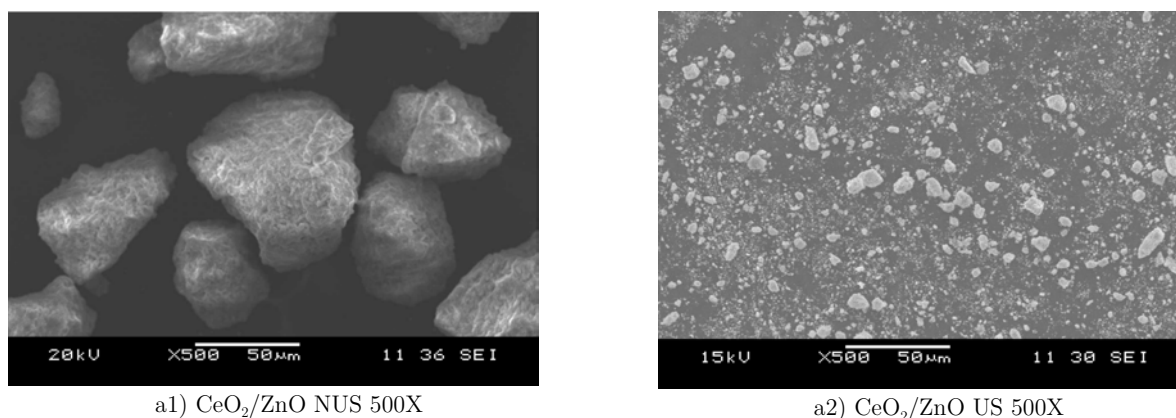


Figure 4. SEM micrographs of NUS and US synthesized CeO_2/ZnO particles respectively, at magnification a1) CeO_2/ZnO NUS 500X; a2) CeO_2/ZnO US 500X

4.5 Transmission Electron Microscopy (TEM)

Figure 5 shows the TEM graphs of the composite CeO_2/ZnO particles generated via US and NUS synthesis respectively. The images clearly confirm the formation of CeO_2/ZnO composite particles, as proposed. The average size of particles as seen in the TEM graphs is in good agreement with the calculated crystallite size from XRD analysis. TEM graphs not only depict the formation of spherical particles, it can be clearly seen that the CeO_2 nanoparticles have been coated with ZnO nanoparticles. The darker portions represent the CeO_2 core, while the lighter area represents the ZnO shell. A fairly narrow size distribution and uniform shape could be observed in the particles synthesized. The average particle size was 8 nm with the average diameter of the CeO_2 core being 6 nm and the average width of the ZnO coating being 2 nm, in case of US synthesized particles. The NUS synthesized particles had an average particle size of 12 nm with the average diameter of the CeO_2 core being 8 nm and the average width of the ZnO coating being 4 nm. From TEM images of NUS synthesized nanoparticles, it can be clearly seen that the individual particles have aggregated to form secondary particles of larger size.

The selected area electron diffraction (SAED) patterns correspond to the CeO_2/ZnO nanoparticles synthesized via US (Fig. 5 a1, a2) and NUS (Fig. 5 b1, b2) techniques. Crystallinity could be observed based on the particles and their corresponding SAED patterns. Both patterns support the formation of a composite material with contribution from both CeO_2 and ZnO evident in the image. The diffused ring patterns correspond to the presence of CeO_2 while presence of crystalline ZnO is evident from more defined spots in the pattern.

4.6 Photocatalytic Activity

Investigation of Photocatalytic Activity:

The photocatalytic activity of the prepared samples was tested for the degradation of RhB constant optimum loading of photocatalyst. The effect of change in the method of synthesis of the photocatalyst on the extent of degradation was investigated and has been discussed in the following sections.

Effect of Preparation method (US and NUS):

Photocatalytic activity of CeO_2/ZnO core-shell photocatalysts synthesized by both US and NUS techniques, was evaluated through the degradation of a basic dye i.e. Rhodamine B in an aqueous solution under UV radiation, as mentioned in the degradation experiment. The removal of Rhodamine B in the presence of catalyst powders prepared via both methods was confirmed by a drop in the absorbance peak within visible wavelength as shown in Figure 6.

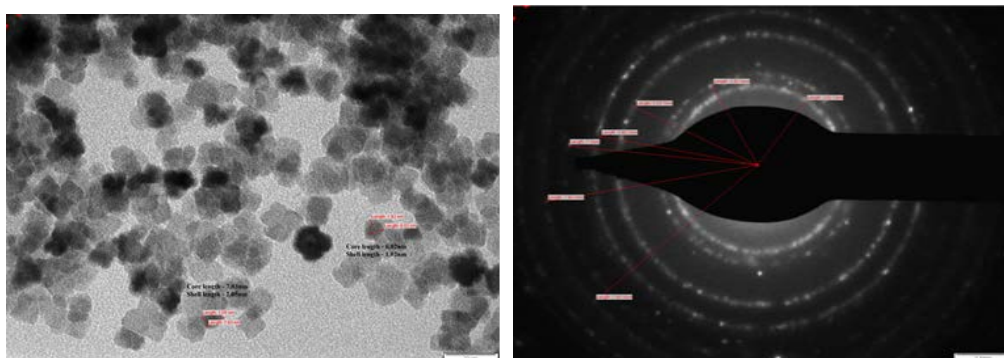


Figure 5. a1, a2: TEM images and SAED pattern of CeO₂/ZnO nanoparticles synthesized by US technique

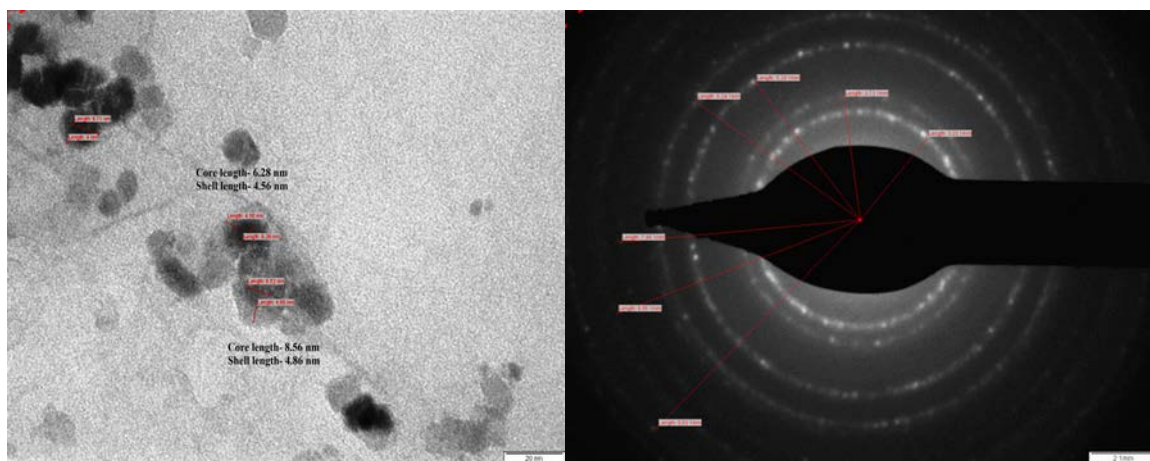


Figure 5. b1, b2: TEM images and SAED pattern of CeO₂/ZnO nanoparticles synthesized by NUS technique

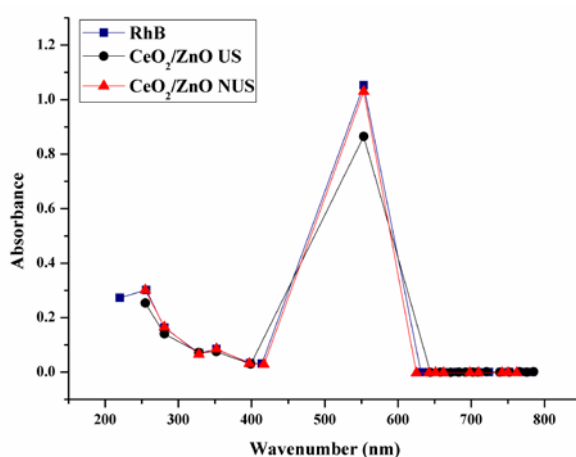


Figure 6. UV-vis spectra of RhB during photocatalytic degradation

It has been reported by Minero et al. [36] that when the alteration of the shape of the spectrum is not significant, it indicates that there is no colored degradation intermediates produced. Thus, the spectral

interference during our reaction was negligible and the change in absorbance value can be due to dye degradation in presence of photocatalyst, after 90 mins. The concentration of Rhodamine B was detected at its maximum absorbance of 554 nm as found from the absorption peak in Figure 7.

The degradation efficiency of Rhodamine B is defined as follows:

$$\text{Degradation efficiency (\%)} = (C_0 - C_t)/C_0 \times 100 \dots\dots\dots (\text{Eq. 2})$$

Where C_0 is the initial concentration of Rhodamine B and C_t is the concentration of Rhodamine B at reaction time t (min). Figure 8 shows the comparison of degradation efficiency Rhodamine B in the presence of the synthesized nano-sized powders, under UV radiation at different moments. It can be seen that the absorption peaks of Rhodamine B solutions gradually decrease along with irradiation time, which indicates that Rhodamine B in aqueous solutions is decomposed under UV light.

The detailed degradation processes are shown in Figure 8. It could be seen that the degradation ratio of Rhodamine B in the presence of nano-sized CeO_2/ZnO synthesized via US technique, powder attains 62.71% within 90 minutes of exposure to UV light, while it was 55.56% for Rhodamine B in presence of CeO_2/ZnO synthesized from NUS technique, for similar experimental conditions. Correspondingly, the degradation ratio of Rhodamine B in the absence of any catalyst under only UV irradiation was only 7.05%, for similar experimental conditions.

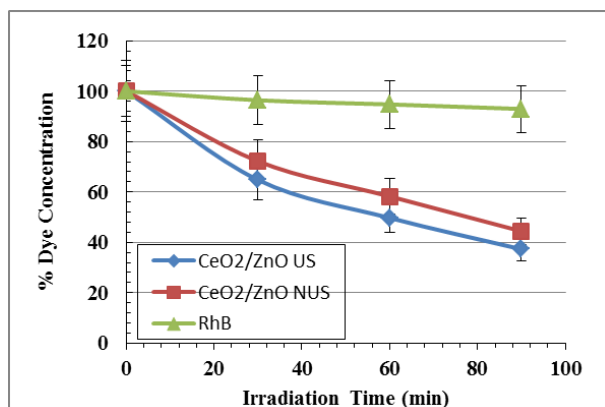


Figure 7. Degradation of RhB with respect to time in presence of photocatalyst

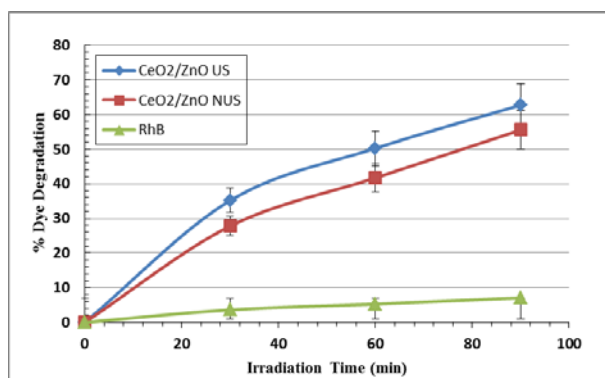


Figure 8. Effect of photocatalyst on degradation of RhB

Irradiation of metal oxide particles with photons of energy equal to or greater than their band gap energy, results in the promotion of an electron from the valence band (VB) to the conduction band (CB) of the particle. The outcome of this process is a region of positive charged hole, in the valance band. The charge can migrate to the particle surface, where the holes can react with surface-bound hydroxyl groups (OH^-) and adsorbed water molecules to form hydroxyl radicals ($\text{OH}\cdot$) ie carry out water

dissociation reaction. The high intensity of UV light generated in the reactor leads to generation of large amount of free radicals in the aqueous system, hence causing an increased degradation.

In addition, to infer the reaction kinetics of photocatalytic degradation of Rhodamine B, the data of $-\ln(C_t/C_0)$ for first-order reaction as a function of irradiation time (t) were calculated. Fig.9 indicates that all calculated values of $-\ln(C_t/C_0)$ are approximately linear with the irradiation time all through for photocatalytic degradation of Rhodamine B for all cases; i.e. they conform to pseudo first-order kinetics reactions. Nevertheless, the rate constants of photodegradation processes of rhodamine B in presence of US synthesized CeO_2/ZnO and NUS synthesized CeO_2/ZnO composite nanoparticles are much larger than that of photodegradation of RhB solution without catalysts. This supports our intention for synthesis of photocatalytic materials for degradation of RhB dye.

The photocatalytic activities of these nanoparticles show significant differences. That is, the order of photocatalytic activities is US synthesized CeO_2/ZnO > NUS synthesized CeO_2/ZnO . The corresponding degradation ratios calculated are 62.71% and 55.56% respectively, and that the degradation ratio under UV radiation alone is only 7.05%. These results clearly support the superiority of CeO_2/ZnO core-shell particles synthesized via US technique, as photocatalysts, over those synthesized via NUS technique.

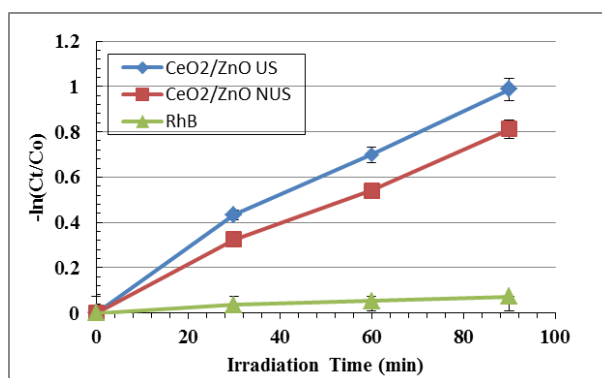


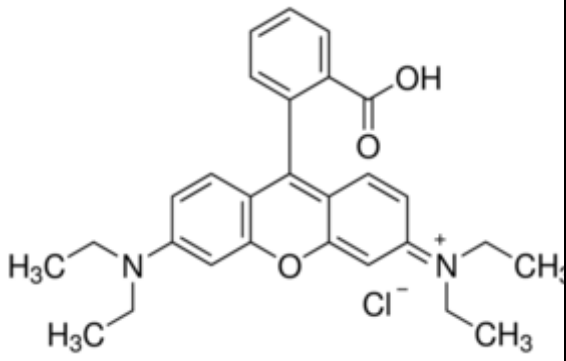
Figure 9. Influence of photocatalyst on rate of degradation of RhB

5 Conclusions

CeO_2/ZnO composite nanoparticles with core-shell morphology were successfully synthesized via precipitation method. Both the techniques were effectively utilized to synthesize CeO_2/ZnO core-shell particles of nanosize, as evident from the SEM and TEM analysis. US synthesized particles also exhibit smaller crystallite size as compared to NUS synthesized particles as reported by XRD analysis. The catalysts prepared via US synthesis exhibited higher catalytic degradation towards Rhodamine B dye as compared to NUS particles, as observed during the degradation experiment of RhB because of the smaller particle size of US assisted technique. Ultrasound-assisted technique (US) also saved substantial amount of energy (more than 80%) during the synthesis of CeO_2/ZnO core-shell catalyst. Thus the ultrasound-assisted method is a simple, convenient, time saving, economical and environmentally benign technique to synthesize nanoparticles with core-shell morphology and the particles exhibited by this method depict superior photocatalytic activity.

Dye:

Common name	Rhodamine B
Class	Xanthenes
Solubility	Soluble
Empirical	$\text{C}_{28}\text{H}_{31}\text{ClN}_2\text{O}_3$

Structure	
Molecular weight	479.02
Max	554 nm

References

1. L. Kong, X.Gan, A.Ahmad, B.Hamed, E.R.Evarts, B.Ooi, J.Lima, Design and synthesis of magnetic nanoparticles augmented microcapsule with catalytic and magnetic bifunctionalities for dye removal, *Chem.Eng. J.* 197(2012) 350–358.
2. F.C. Wu, R.L.Tseng, High adsorption capacity NaOH-activated carbon for dye removal from aqueous solution, *J.Hazard.Mater.* 153(2007) 1256–1267.
3. R. Aparna, A. Hameed, Z.H. Yamani, K.S. Rakesh, Synthesis and photocatalytic activity of nano-sized iron oxides, *Journal of Hazardous Materials* 102 (2003) 231.
4. S. Tsunekawa, R. Sahara, Y. Kawazoe, A. Kasuya, Origin of the blue shift in ultraviolet absorption spectra of nanocrystalline CeO₂ particles, *Mater. Trans. JIM* 41 (2000) 1104–1107.
5. A. Trovarelli, C. de Leitenburg, M. Boaro, G. Dolcetti, The utilization of ceria in industrial catalysis, *Catal. Today* 50 (1999) 353–367.
6. Yue Lin, Zhang Xiaoming, Preparation of highly dispersed CeO₂/TiO₂ core-shell nanoparticles, *material letters* 62 (2008) 3764–3766.
7. I-Tsan Liua, Min-Hsiung Hona, Lay Gaik Teoh, The preparation, characterization and photocatalytic activity of radical-shaped CeO₂/ZnO microstructures, *Ceramics International*, 2013.
8. Ni Huang, Jinxia Shu, Zhonghua Wang, Ming Chen, Chunguang Ren, Wei Zhang, One-step pyrolytic synthesis of ZnO nanorods with enhanced photocatalytic activity and high photostability under visible light and UV light irradiation, *Journal of Alloys and Compounds* Volume 648, 5 November 2015, Pages 919–929.
9. Yu Miao, Haijiao Zhang, Shuai Yuan, Zheng Jiao, Xuedong Zhu, Preparation of flower-like ZnO architectures assembled with nanosheets for enhanced photocatalytic activity, *Journal of Colloid and Interface Science* Volume 462, 15 January 2016, Pages 9–18.
10. G. Poongodi, P. Anandan, R. Mohan Kumar, R. Jayavel, Studies on visible light photocatalytic and antibacterial activities of nanostructured cobalt doped ZnO thin films prepared by sol-gel spin coating method, *Spectrochimica Acta Part A: Molecular and Biomolecular Spectroscopy* Volume 148, 5 September 2015, Pages 237–243.
11. Olfa Bechambi, Manel Chalbi, Wahiba Najjara, Sami Sayadi, Photocatalytic activity of ZnO doped with Ag on the degradation of endocrine disrupting under UV irradiation and the investigation of its antibacterial activity, *Applied Surface Science*, Volume 347, 30 August 2015, Pages 414–420.
12. Chaorong Li, , Rui Chen, Xiaoqiang Zhang, Shunxin Shu, Jie Xiong, Yingying Zheng, Wenjun Dong, Electrospinning of CeO₂-ZnO composite nanofibers and their photocatalytic property, *Materials Letters*. Volume 65, Issue 9, 15 May 2011, Pages 1327–1330.
13. Qingshui Xie, Yue Zhao, Huizhang Guo, Aolin Lu, Xiangxin Zhang, Laisen Wang, Ming-Shu Chen, and Dong-Liang Peng, Facile Preparation of Well-Dispersed CeO₂-ZnO Composite Hollow Microspheres with Enhanced Catalytic Activity for CO Oxidation, *ACS Appl. Mater. Interfaces*, 2014, 6 (1), pp 421–428.

14. S. Prabhu, T. Viswanathan, K. Jothivenkatachalam, and K. Jeganathan, Visible Light Photocatalytic Activity of CeO₂-ZnO-TiO₂ Composites for the Degradation of Rhodamine B, *Indian Journal of Materials Science*, Volume 2014 (2014).
15. A.V. Rajgure, N.L. Tarwal, J.Y. Patil, L.P. Chikhale, R.C. Pawar, C.S. Lee, I.S. Mulla, S.S. Suryavanshi, Gas sensing performance of hydrothermally grown CeO₂-ZnO composites, *Ceramics International*, <http://dx.doi.org/10.1016/j.ceramint.2013.11.025>
16. I-Tsan Liu, Min-Hsiung Hon, Lay Gaik Teoh, The preparation, characterization and photocatalytic activity of radical-shaped CeO₂/ZnO microstructures, <http://dx.doi.org/10.1016/j.ceramint.2013.08.053>
17. Yongjun He, Xiangyang Yu, Tianliang Li, Lanying Yan, Bolun Yang, Preparation of CeO₂/ZnO nanostructured microspheres and their catalytic properties, *Powder Technology* 166 (2006) 72–76.
18. A.M. Torres-Huerta, M.A. Domínguez-Crespo, S.B. Brachetti-Sibaja, H. Dorantes-Rosales, M.A. Hernández-Pérez, J.A. Lois-Correa, Preparation of ZnO:CeO₂ thin films by AP-MOCVD: structural and optical properties, *Journal of Solid State Chemistry*, 183(2010) 2205–2217.
19. T.Y. Ma, Z.Y. Yuan, J.L. Cao, Hydrangea-like meso/macroporous ZnO–CeO₂ binary oxide materials: synthesis, photocatalysis and CO oxidation, *European Journal of Inorganic Chemistry* 5(2010)716–724.
20. R. Li, S. Yabe, M. Yamashita, S. Momose, S. Yoshida, S. Yin, T. Sato, Synthesis and UV-shielding properties of ZnO- and CaO-doped CeO₂ via soft solution chemical process, *Solid State Ionics* 151(2002) 235–241.
21. Y. He, X. Yu, T. Li, L. Yan, B. Yang, Preparation of CeO₂/ZnO nanostructured microspheres and their catalytic properties, *Powder Technology* 166(2006) 72–76.
22. J.F. de Lima, R.F. Martins, C.R. Neri, O.A. Serra, ZnO:CeO₂-based nanopowders with low catalytic activity as UV absorbers, *Applied Surface Science* 255(2009)9006–9009.
23. L.Y. Mo, X.M. Zheng, C.T. Yeh, A novel CeO₂/ZnO catalyst for hydrogen production from the partial oxidation of methanol, *Chem- Phys Chem* 6(2005) 1470–1472.
24. N. Perkas, G. Amirian, C. Rottman, F. de la Vega, A. Gedanken, Sonochemical deposition of magnetite on silver nanocrystals, *Ultrason. Sonochem.* 16(2009)132–135.
25. N. Ghows, M.H. Entezari, Sono-synthesis of core-shell nanocrystal (CdS/TiO₂) without surfactant, *Ultrason. Sonochem.* 19(2012) 1070–1078.
26. M.S.T. Gonsalves, A.M.F. Oliveira-Campos, E.M.M.S. Pinto, P.M.S. Plasencia, M.J.R.P. Queiroz, Photochemical treatment of solutions of azo dyes containing TiO₂, *Chemosphere* 39 (1999) 781–786.
27. R. Nagaraja, Nagaraju Kottam, C.R. Girija, B.M. Nagabhushana; Photocatalytic degradation of Rhodamine B dye under UV/solar light using ZnO nanopowder synthesized by solution combustion route *Powder Technology* 215-216 (2012) 91–97.
28. Balvant S. Singh, Hyacintha R. Lobo, Dipak V. Pinjari, Krishna J. Jarag, Aniruddha B. Pandit, Ganapati S. Shankarling, Comparative material study and synthesis of 4-(4-nitrophenyl)oxazol-2-amine via sonochemical and thermal method, *Ultrasonics Sonochemistry* 20 (2013) 633–639.
29. K.J. Jarag, D.V. Pinjari, A.B. Pandit, G.S. Shankarling, Synthesis of chalcone (3-(4-fluorophenyl)-1-(4-methoxyphenyl)prop-2-en-1-one): Advantage of sonochemical method over conventional method, *Ultrasonics Sonochemistry* 18 (2011) 617–623.
30. S.E. Karekar, B.A. Bhanvase, S.H. Sonawane, M.P. Deosarkar, D.V. Pinjari, A.B. Pandit, Synthesis of zinc molybdate and zinc phosphomolybdate nanopigments by an ultrasound assisted route: Advantage over conventional method, *Chemical Engineering and Processing* 87 (2015) 51–59.
31. M.A. Patel, B.A. Bhanvase, S.H. Sonawane, Production of cerium zinc molybdate nano pigment by innovative ultrasound assisted approach, *Ultrasonics Sonochemistry* 20 (2013) 906–913.
32. S.G. Anju, Suguna Yesodharan, E.P. Yesodharan, Zinc oxide mediated sonophotocatalytic degradation of phenol in water; *Chemical Engineering Journal* 189–190 (2012) 84–93.
33. K. Prasad, D.V. Pinjari, A.B. Pandit, S.T. Mhaske, Phase transformation of nanostructured titanium dioxide from anatase-to-rutile via combined ultrasound assisted sol-gel technique, *Ultra Sonochem.* 17 (2010) 409–415.
34. N. Enomoto, T. Koyano, Z. Nakagawa, Effect of ultrasound on synthesis of spherical silica, *Ultra Sonochem.* 3 (1996) S105–S109.
35. R.L. Frost, M. Daniel Lisa, Z. Huaiyong, Synthesis and characterization of clay supported titania photocatalysts, *J. Colloid Int. Sci.* 316 (2007) 72–79.
36. C. Minero, P. Pellizzari, V. Maurino, E. Pelizzetti, D. Vione, *Appl. Catal. B: Environ.* 77 (2008) 308–316.